CFD Modeling of Air Cooling of Multiple Beef Carcasses Using 3D Geometrical Models

Article *in* Acta horticulturae · October 2013

DOI: 10.17660/ActaHortic.2013.1008.20

CITATION
1

READS
147

8 authors, including:

Thijs Defraeye
Empa - ETHZ
82 PUBLICATIONS **993** CITATIONS
SEE PROFILE

Bart Nicolaï
University of Leuven
647 PUBLICATIONS **8,133** CITATIONS
SEE PROFILE

Stefaan De Smet
Ghent University
262 PUBLICATIONS **4,326** CITATIONS
SEE PROFILE

Pieter Verboven
University of Leuven
329 PUBLICATIONS **3,513** CITATIONS
SEE PROFILE

CFD Modeling of Air Cooling of Multiple Beef Carcasses Using 3D Geometrical Models

Kumsa Kuffi[1], Thijs Defraeye[1], Erwin Koninckx[3,4], Stefaan Lescouhier[2], Bart M. Nicolaï[1], Stefaan De Smet[2], Annemie Geeraerd[1], Pieter Verboven[1]

[1] BIOSYST-MeBioS, Katholieke Universiteit Leuven, Willem de Croylaan 42, B-3001, Leuven, Belgium

[2] Laboratory for Animal Nutrition and Animal Product Quality, Ghent University, Proefhoevestraat 10, 9090 Melle, Belgium

[3] Flemish Cycling Federation, Globelaan 49/2, 1190 Brussels, Belgium

[4] Research Centre for Exercise and Health, Department of Biomedical Kinesiology, Katholieke Universiteit Leuven, Tervuursevest 101, 3001 Heverlee, Belgium

Keywords : Turbulence modeling, meat, surface heat transfer coefficient, laser scan,chilling

Abstract

Fast cooling of beef carcasses has an important effect on reducing color instability in the deep muscles of the carcass. A numerical simulation of beef carcass chilling was done by using a digital scan of beef carcass geometry and measured values of flow properties. The scanning process and measurement were conducted in an industrial chiller to obtain realistic working condition for the simulation input. Simulation of 60h chilling was performed for a single and multiple carcasses. Simulation results were validated with measurements and the effect of flow direction on the cooling rate was analyzed.

INTRODUCTION

After slaughter, meat undergoes various biochemical and physiological changes which leads to quality degradation of the product. The rate of these changes can be controlled by fast chilling of the beef carcass. Color instability which is usually observed in the internal part of the beef carcass occurs due to the biochemical and physiological changes taking place in meat at high temperature and relatively low pH (James and James, 2002). Fast cooling of the internal parts of beef carcasses just after slaughter has been shown to be beneficial in maintaining color stability and a more stable product. The rate of cooling depends on cooling air properties like temperature, humidity, air velocity and turbulence as well as carcass geometric properties such as size and shape.

Apart from experiments, optimization of carcass cooling can also be done using CFD. Trujillo and Pham (2006) and Pham et al. (2009) presented a CFD modeling approach with RNG low-Reynolds number wall treatment to predict the convective air cooling of a single beef carcass using a 3D geometrical model assembled from cross sectional images. Mirade and Picgirard (2001) showed that CFD can be used to optimize airflow distribution in carcass cool rooms and used simplified carcass geometries to perform large scale computations.

In this study, air flow measurements of cooling air were conducted in an industrial beef carcass chiller and the carcass geometry was obtained using 3D surface scanning. This information was used to provide realistic input for the numerical simulations. Carcass temperatures at different positions and depths were measured for validating the simulation result.

The aim of this contribution was to see the effect of flow directions on cooling rate of multiple beef carcasses using a CFD model with a realistic carcass geometry obtained from a laser scan, and to compare with a single carcass.

MATERIALS AND METHODS

Measurements

Air velocities were measured with an ultrasonic anemometer (Gill WindMaster, Gill Instruments Ltd, Hampshire, England) at 32 Hz sampling rate at 8 different positions around the carcass to obtain velocity and turbulence intensity values, in order to determine realistic boundary conditions of the computational domain (Fig.1b). Carcass temperatures were measured on leg and rib locations at different depth for about 72h with thermometers connected to data loggers. The humidity and temperature of the air were measured, for the same duration, with humidity sensors having data logging facility.

Modeling and Simulation

A digital model of the carcass was obtained using a high-resolution 3D laser scanning system (K-Scan, Nikon Metrology, Belgium), capturing the specific body characteristics of the carcass (Fig.1a). From the 3D virtual carcass model, computational domains with dimension of (18 m X 8 m X 5.5 m) were developed by ANSYS Design Modeler for single and multiple carcasses. Unstructured meshing of 1.8 and 2.5 million elements for single and multiple carcass computational domains respectively was done by ANSYS ICEM CFD. CFD computations were performed in parallel with ANSYS CFX on a 12-core 2.66GHz 48GB RAM PC. The measured cooling air average velocity(0.58ms^-1), temperature(2.3°C), relative humidity(100%) and turbulence intensity at measurement points were used as model input for the simulation. Measured carcass temperatures were used for validation of experimental values with the simulation results.

The cooling of beef carcass is achieved by heat exchange with the environment, i.e. the cooling media (air) surrounding it. This heat is transported through the carcass by conduction and then removed at the surface by convection, evaporation and radiation. The process involves the transfer of heat (and mass) from the carcass surface. The heat balance at the carcass surface can be expressed as:

$$-k\frac{\partial T}{\partial n} = h_c(T_s - T_a) + L_v\frac{h_m}{R}\left(\frac{a_\omega P_{w,T_s}}{T_s} - \frac{rhP_{w,Ta}}{T_a}\right) \quad \text{----------} \quad (1)$$

with the surface heat transfer coefficient (W m^{-2} K^{-1}), T_a the air temperature (K), T_s the surface temperature, σ the Stefan-Boltzmann constant (5.67×10^{-8} W $m^{-2}K^{-4}$), ε the emissivity, h_m the surface mass transfer coefficient (m s^{-1}), R the specific gas constant for water (J kg^{-1} K^{-1}), rh

the relative humidity, P_w vapor pressure of water (Pa), a_ω the water activity of carcass surface, L_v the latent heat of vaporization (J kg^{-1}) and k the thermal conductivity of the meat (W m^{-1} °C^{-1}). Inside the beef carcasses (solid domain) the heat transport equation was solved while in the air domain a set of five transport equations (continuity, momentum, heat, turbulent kinetic energy and turbulent dissipation) were solved. At the interface between the solid and the fluid domains the energy flux lose due to evaporation, the second term on the right of equation (1), was included as an energy source for fluid domain. A constant value of the water activity was used in the expression. Heat lose by radiation was not included in the simulation as net radiation energy transfer from one carcass to the other carcass is negligible. For rows of carcasses exposed to the walls of the chilling room this effect may not be negligible during the initial hours of chilling as the wall temperature is lower than the carcass temperature. The convective heat transfer is directly calculated by the software based on flow properties and the geometric shape. Obtaining a realistic geometry therefore helps in calculating convective heat transfer, and the convective heat transfer coefficient, more accurately. For the turbulence modeling, Reynolds-averaged Navier-Stokes (RANS) with the shear stress transport (SST) k-ω model was used (Delele et al., 2008).

RESULTS AND DISCUSSION

Figure 2b, presenting results for a single carcass, shows that the carcass sides cool faster around the ribs as compared to the leg part due to the difference in thickness of each part. On the same figure, during the initial hours of chilling the measured temperature profile increase in the leg but not in the rib. There is more glycogen storage at legs than at ribs, which contributes to heat production in beef muscle during rigor mortis (James and C.James, 2002), which will be thus more pronounced in the thicker parts. Future models should take this heat production into account. Figures 3b and 4b indicate that at the working conditions of the considered industrial chiller, the flow direction doesn't have a considerable effect on the rate of cooling. This can be due to the fact that the conductive heat transfer is mainly controlling the rate of cooling. This is evident from the ratio of the heat transfer resistances inside the carcass to the surface of the carcass (Biot number) which is much larger than 1.

Measured cooling air velocity and calculated turbulence intensity at the measurement points around the carcass is shown on figure 5.

ACKNOWLEDGEMENTS

Flanders' Food and the Belgian slaughter houses are gratefully acknowledged for financial support

References

Delele, M., Tijskens, E., Atalay, Y., Ho, Q., Ramon, H., Nicolaï, B., Verboven, P. (2008). Combined discrete element and CFD modeling of airflow through random stacking of horticultural products in vented boxes. Journal of food engineering, 89 (1), 33-41.

Mirade P.S. and Picgirard L. (2001). Assessment of airflow patterns inside six industrial beef carcass chillers. International Journal of Food Science and Technology 36: 463-475.
Pham, Q.T., Trujillo F.J. and McPhail, N. (2009). Finite element model for beef chilling using CFD-generated heat transfer coefficients. International Journal of Refrigeration 32: 102-113.
S.J. James and C.James, 2002. Meat refrigeration. Wood head, Cambridge, England
Trujillo, F.J. and Pham ,Q.T. (2006). A computational fluid dynamics model of the heat and moisture transfer during beef chilling. International Journal of Refrigeration 29: 998-1009.

Figures

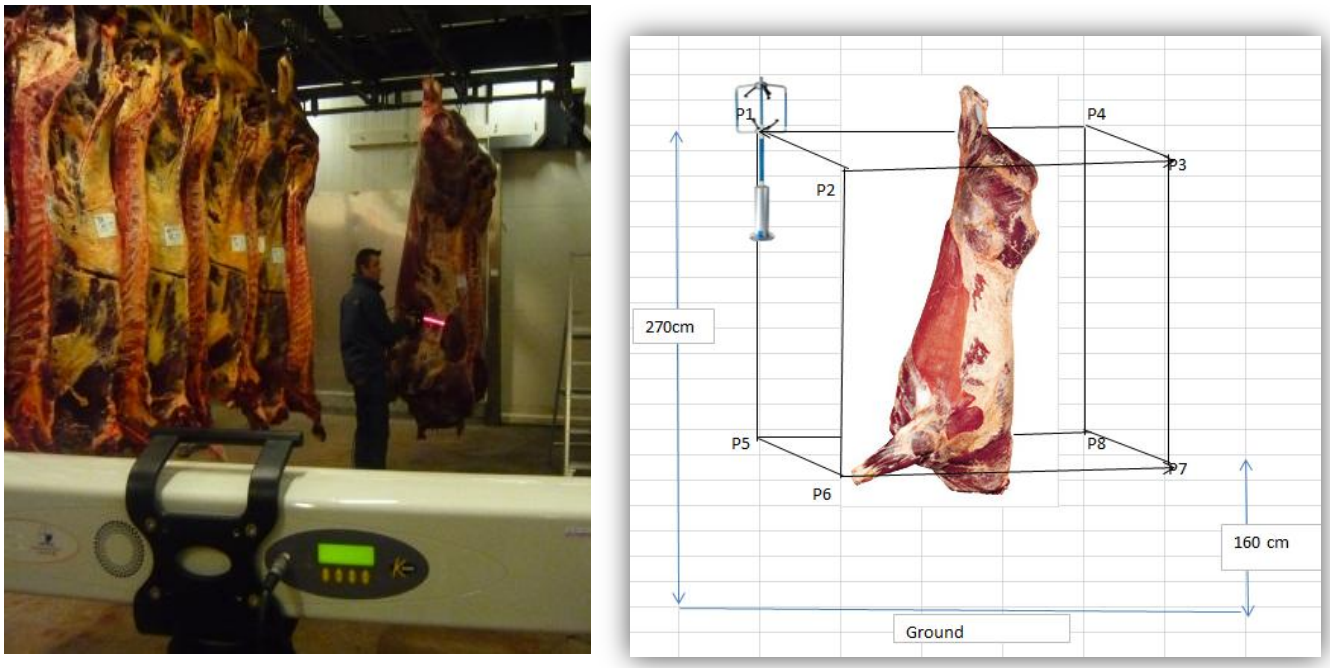

(a) (b)

Fig. 1. Experimental setup for 3D scanning of the carcass (a) and air velocity measurements around beef carcass (b).

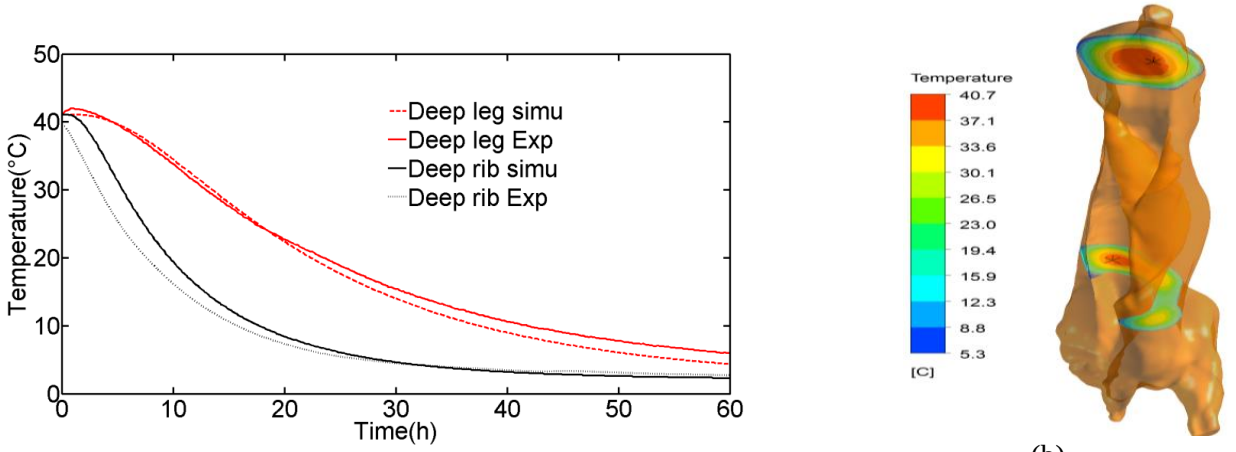

(a) (b)

Fig. 2. (a) Comparison of experimental values of temperature to numerical simulation results at deep leg and rib for horizontal air flow direction through the computational domain containing a single carcass. (b) illustrative temperature contour plot at leg and rib.

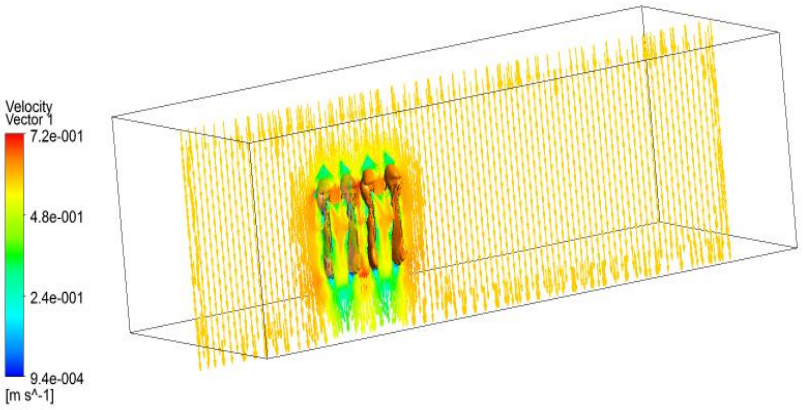

(a)

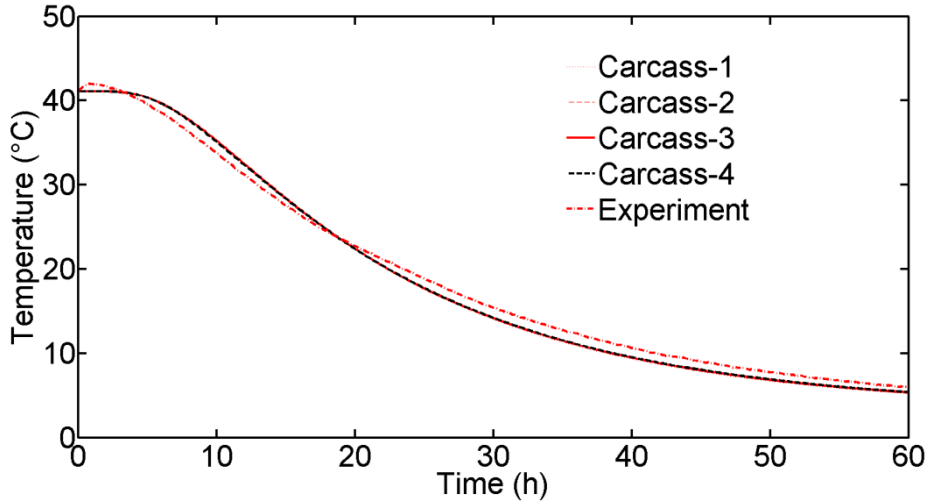

(b)

Fig.3. (b)Comparison of experimental values of temperature with numerical simulation results at deep legs (a)illustrative velocity vector for vertical (downwards) air flow through multiple carcasses.

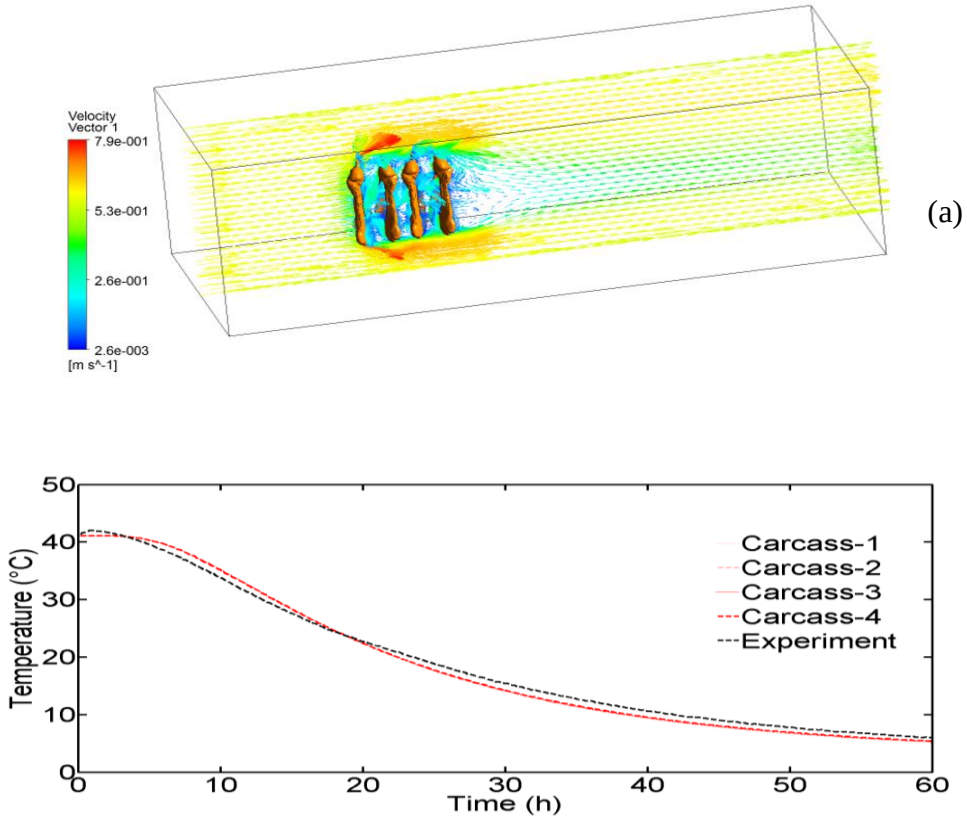

Fig. 4 . (b)Comparison of experimental values of temperature with numerical simulation results at deep legs (a)illustrative velocity vector for horizontal air flow through multiple carcasses.

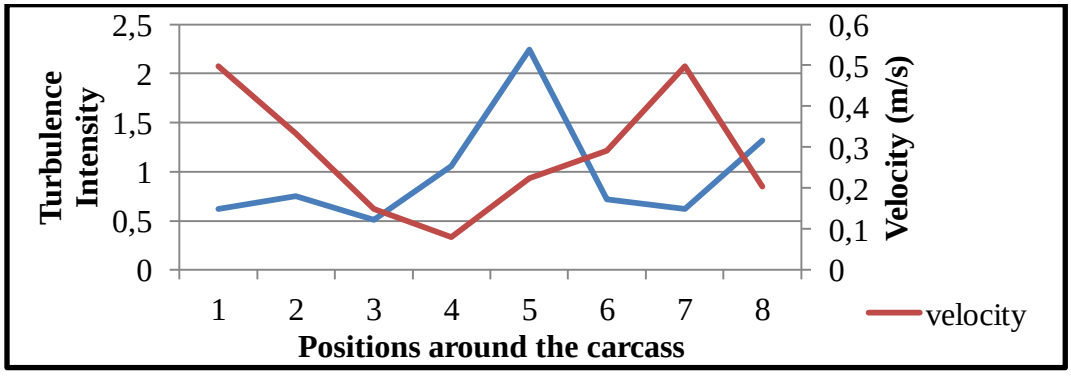

Fig. 5.Turbulence intensity and velocity at mesurement points around the carcass.